Mon. Not. R. Astron. Soc. **383,** L25–L29 (2008) doi:10.1111/j.1745-3933.2007.00403.x

Relativistic jets and long-duration gamma-ray bursts from the birth of magnetars

N. Bucciantini,[1★] E. Quataert,[1] J. Arons,[1,2,3] B. D. Metzger[1,2] and T. A. Thompson[4]†

[1] *Astronomy Department and Theoretical Astrophysics Center, University of California, Berkeley, 601 Campbell Hall, Berkeley, CA 94720, USA*
[2] *Department of Physics, University of California, Berkeley, Le Conte Hall, Berkeley, CA 94720, USA*
[3] *Kavli Institute for Particle Astrophysics and Cosmology, Stanford University, Menlo Park, CA 94025, USA*
[4] *Department of Astrophysical Sciences, Peyton Hall, Ivy Lane, Princeton, NJ 08544, USA*

Accepted 2007 September 26. Received 2007 August 30; in original form 2007 July 13

ABSTRACT

We present time-dependent axisymmetric magnetohydrodynamic simulations of the interaction of a relativistic magnetized wind produced by a proto-magnetar with a surrounding stellar envelope, in the first ∼10 s after core collapse. We inject a super-magnetosonic wind with $\dot{E} = 10^{51}$ erg s^{-1} into a cavity created by an outgoing supernova shock. A strong toroidal magnetic field builds up in the bubble of plasma and magnetic field that is at first inertially confined by the progenitor star. This drives a jet out along the polar axis of the star, even though the star and the magnetar wind are each spherically symmetric. The jet has the properties needed to produce a long-duration gamma-ray burst (GRB). At ∼5 s after core bounce, the jet has escaped the host star and the Lorentz factor of the material in the jet at large radii $\sim 10^{11}$ cm is similar to that in the magnetar wind near the source. Most of the spindown power of the central magnetar escapes via the relativistic jet. There are fluctuations in the Lorentz factor and energy flux in the jet on a ∼ 0.01–0.1 s time-scale. These may contribute to variability in GRB emission (e.g. via internal shocks).

Key words: magnetic fields – MHD – stars: neutron – supernovae: general – stars: winds, outflows – gamma-rays: bursts.

1 INTRODUCTION

Observations of long-duration gamma-ray bursts (GRBs) show that many are associated with core-collapse supernovae (SNe) (Woosley & Bloom 2006). Newly formed rapidly rotating magnetars (e.g. Usov 1992; Thompson 1994; Wheeler et al. 2000) or black holes with an accretion disc (e.g. MacFadyen & Woosley 1999) are possible central engines powering GRBs and their associated SNe. In both of these models, a key problem is to understand how the relativistic material necessary for generating the GRB escapes from deep within the host star. A natural possibility, suggested by both afterglow observations (‘jet breaks’; Rhoads 1999) and GRB energetics, is that a collimated outflow punches through the stellar envelope, providing a channel out of which the relativistic material can escape (e.g. Matzner 2003).

In the collapsar model, collimated outflows from GRBs are accounted for by jets produced by an accretion flow on to a central black hole. In the magnetar model, the origin of such collimated outflows is less clear because relativistic outflows by themselves do not efficiently self-collimate (e.g. Lyubarsky & Eichler 2001). Königl & Granot (2002) suggested, by analogy to pulsar wind nebulae (Begelman & Li 1992) (PWNe), that the interaction of the wind from the spinning-down magnetar with the surrounding star could facilitate collimation. In a previous paper, we used axisymmetric thin-shell calculations to demonstrate that this can in fact occur [Bucciantini et al. 2007; see Uzdensky & MacFadyen (2006, 2007) for related ideas based on force-free rather than inertially loaded outflows]. As Königl & Granot anticipated, the physical picture is analogous to that used to understand the morphologies of PWNe (Komissarov & Lyubarsky 2004; Del Zanna, Amato & Bucciantini 2004): the magnetar wind shocks on the surrounding (exploding) stellar envelope, creating a bubble of relativistic plasma and magnetic field inside the host star (a ‘magnetar wind nebula’, or MWN). If the toroidal magnetic field in the bubble is sufficiently strong, the bubble expands primarily in the polar direction owing to the ‘tube of toothpaste’ effect – the magnetic hoop stress in the equator creates a pressure gradient along the axis which is not balanced by any restoring force, thus driving the flow preferentially in the polar direction. The nebula itself is ultimately confined by the inertia of the SN envelope, to which little energy is transferred, in contrast to the pressure confinement in traditional magnetic tower models (Sherwin & Lynden-Bell 2007) or the case of confinement

★E-mail: nbucciantini@astro.berkeley.edu
†Lyman Spitzer Jr Fellow.

by a pressurized cocoon inside the progenitor star (Uzdensky & MacFadyen 2006).

Our previous results were based on a thin-shell model for the interaction between a magnetar wind and its host star. In this Letter, we build on this work by carrying out time-dependent axisymmetric magnetohydrodynamic (MHD) simulations of the interaction between a magnetar wind and a surrounding star. This Letter is organized as a proof of principle to show that a mechanism developed in the PWN context to explain the origin of observed jet/plume features can also apply to proto-magnetars. For this reason we have selected a simplified set of parameters, deferring a detailed parameter study to future work.

We assume that an outgoing SN shock has already created a central evacuated cavity and that the host star is spherically symmetric. A magnetar is assumed to inject energy at a constant rate of $\dot{E} = 10^{51}$ erg s^{-1}, a spindown power that is appropriate for proto-magnetars with $P \sim 1$ ms and $B \sim 10^{15}$ G (e.g. Metzger, Thompson & Quataert 2007). The interaction between the magnetar wind and the host star depends on the strength of the toroidal magnetic field B in the MWN; this in turn depends on the magnetization in the wind at large radii, $\sigma = r^2 B^2 c/\dot{E}$. More specifically, $\sigma(R_{\rm TS}) = \sigma_{\rm TS}$, the magnetization at radii typical of the termination shock radius $R_{\rm TS}$, is the essential control parameter. At early times after core bounce ($\lesssim$ a few seconds), young magnetars lose significant amounts of mass to a neutrino-driven wind, leading to $\sigma_{\rm LC} \lesssim 1$, where $\sigma_{\rm LC}$ is the magnetization evaluated at the light-cylinder. However, the mass-loss rate decreases as the neutron star cools and the wind at later times ($\sim$ 10–100 s) is ultra-relativistic with $\sigma_{\rm LC} \sim 10^2$–$10^3$ (Thompson, Chang & Quataert 2004; Metzger, Thompson & Quataert 2007). This late-time outflow is the most promising for producing a GRB. The relation between $\sigma_{\rm LC}$ – which can be calculated with some confidence – and σ at larger radii in the wind is difficult to determine because of uncertainties in the conversion of magnetic energy into kinetic energy in relativistic winds [see Bucciantini et al. (2007) for a detailed discussion of this problem in the current context]. In this Letter we focus on later times when $\sigma_{\rm LC}$ is large. We assume that non-ideal MHD processes analogous to those that operate in the pulsar–PWN problem are also at work in proto-magnetar winds; these convert the high-$\sigma_{\rm LC}$ wind at the light-cylinder into a moderate-$\sigma_{\rm TS}$, high-γ (lorentz factor) wind at the free wind termination radius. Specifically, we consider relativistic winds with $\gamma_{\rm w} = 10$ or 25 and $\sigma_{\rm TS} = 0.1$; GRBs require somewhat higher γ outflows but these are more difficult to simulate for numerical reasons.

The remainder of this Letter is organized as follows. In the next section (Section 2) we describe our numerical setup. We then present the results of our simulations (Section 3) and discuss their implications for models of GRBs (Section 4).

2 NUMERICAL SETUP

All of the simulations were performed using the shock-capturing central-scheme for relativistic ideal MHD developed by Del Zanna & Bucciantini (2002) and Del Zanna, Bucciantini & Londrillo (2003), using an ideal gas equation of state with adiabatic coefficient 4/3. We refer the reader to these papers for a detailed description of the equations and the numerical algorithms.

The interaction of the magnetar wind with the surrounding SN progenitor was investigated by performing 2D axisymmetric simulations on a spherical grid. The domain in θ is the first quadrant from $\theta = 0$ to $\theta = \pi/2$, with reflecting boundary conditions for v_θ and B at the polar axis to enforce axisymmetry, and similar boundary conditions in the equatorial plane. The grid is uniform in the θ-direction with 100 cells. Given that one needs to study a wide range of spatial scales, from the termination shock at $\sim 10^8$ cm to the outer edge of the star at $\sim 2 \times 10^{10}$ cm, we chose a grid that is logarithmic in radius and that extends from $r_{\rm min} = 10^7$ cm to $r_{\rm max} = 5 \times 10^{10}$ or 10^{11} cm, with 100 cells per decade in radius. Zeroth-order extrapolation is assumed at the outer boundary. The code is second-order in both space and time, with a monotonized central limiter, chosen in order to resolve the large density jump between the lighter relativistic plasma inside the MWN and the heavier stellar envelope (the density can increase by a factor of $\sim 10^4$).

For proto-magnetars with millisecond rotation periods, the location of the Alfvénic surface is at $\sim 10^7$ cm and the fast magnetosonic surface is at $\sim 10^7$– 10^8 cm (Bucciantini et al. 2006, hereafter B06). In the present simulations, we do not attempt to resolve the dynamics of the wind in the sub-magnetosonic region close to the neutron star. Instead, at $r_{\rm min}$ we inject a super-magnetosonic wind with a fixed Lorentz factor of $\gamma_{\rm w} = 10$ or 25 and a magnetization of $\sigma = 0.1$, a value appropriate to distances of the order of the termination shock radius (the simulations were less stable for higher σ); under these assumptions, σ is conserved throughout the upstream region. The wind is assumed to be cold with $\rho c^2/p = 100$ (where ρ is the density, p the pressure and c the speed of light), and to contain a purely toroidal magnetic field. The energy flux $\dot{E} = 10^{51}$ erg s^{-1} is kept constant during the entire simulation. For simplicity, we neglect latitudinal variations in the wind and assume that it is isotropic. Self-consistency requires that the termination shock produced by the interaction of the magnetar wind with the surrounding star and MWN lies at $\gtrsim r_{\rm min}$. If not, the assumption of a super-magnetosonic wind would not be valid. We discuss this constraint more in the next section.

We use a 35-M$_\odot$ stellar progenitor from Woosley, Heger & Weaver (2002). The wind is injected inside a cavity of radius $\sim 10^9$ cm, which is roughly the size of the collapsing region in the first second after core bounce (our initial time). In order to simulate the effect of a SN shock propagating inside the progenitor, the region between 10^9 and 2×10^9 cm is given an outward velocity corresponding to a total kinetic energy $\sim 2 \times 10^{51}$ erg, similar to that used in the 1D explosion calculations of Woosley & Weaver (1995). The surface of the progenitor star is located at 2.5×10^{10} cm. We assume that the density outside the star falls off as r^{-2}; for the range of radii we simulate, the results are independent of the outer density profile.

3 RESULTS

Fig. 1 shows the density, pressure, flow velocity and flow streamlines for our simulations with $\gamma_{\rm w} = 10$ at three different times, 4, 5 and 6 s after core bounce. At all times there is an axial high-velocity jet subtending a few degrees surrounded by a somewhat less relativistic cocoon subtending $\sim 10^\circ$. The jet carries a significant fraction of the spindown energy of the magnetar. Recall that the energy input in the simulation is spherically symmetric, as is the progenitor star. The aspherical evolution of the system is generated self-consistently by the dynamics of the MWN created inside the star. Note that the boundary between the MWN and the host star is particularly easy to identify via the jump in the pressure.

To help explain the physical origin of the jet in Fig. 1, Fig. 2 zooms in and shows the flow velocity and streamlines in the inner region ($\lesssim 4 \times 10^9$ cm) at 4 s. The high-velocity $v \approx c$ region at small radii in Fig. 2 (indicated in red) is the freely expanding wind with $\gamma_{\rm w} = 10$. The wind goes through a termination shock at $\sim 10^8$ cm due to

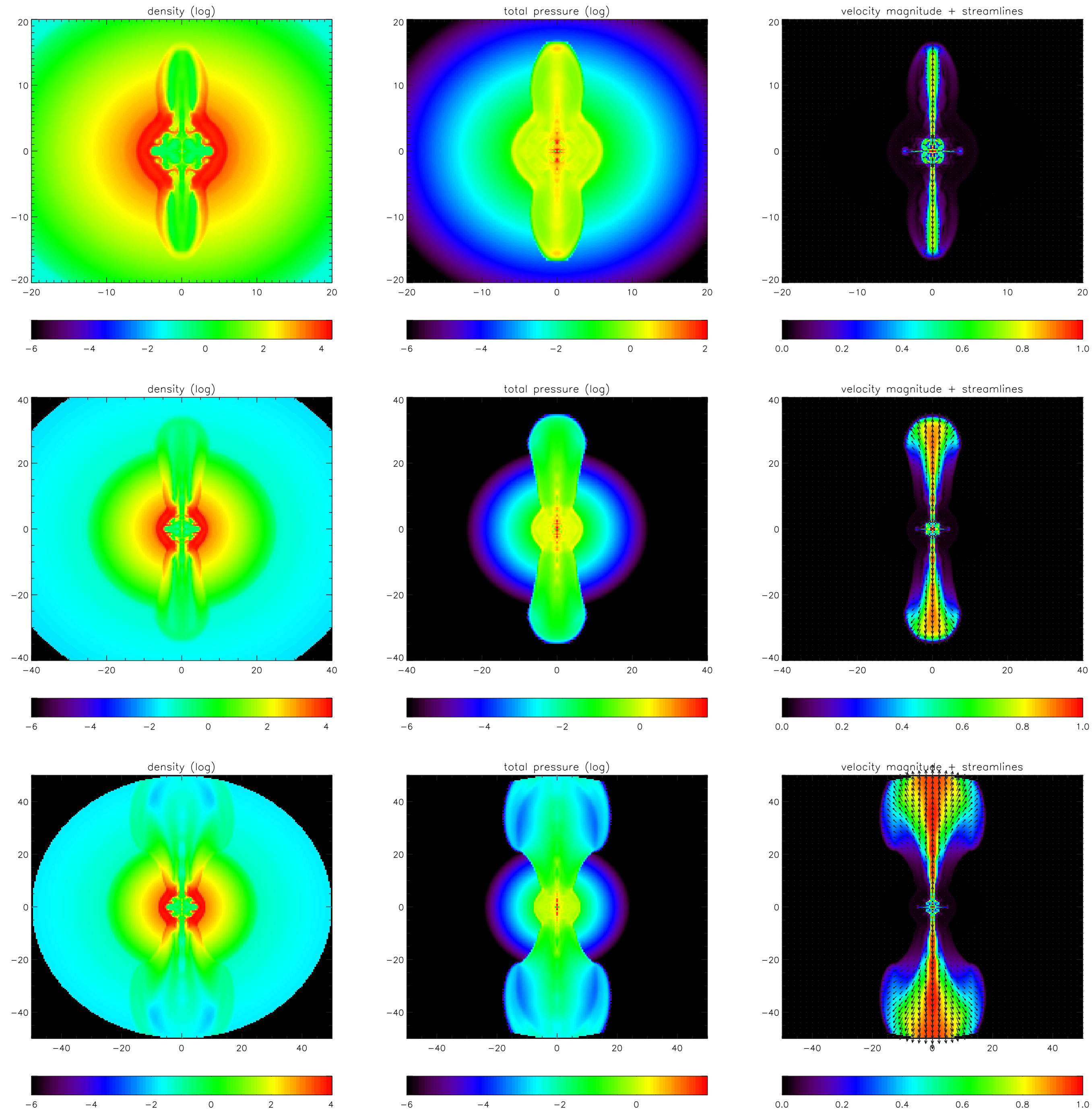

Figure 1. Evolution of a magnetized bubble inflated by a magnetar wind with $\dot{E} = 10^{51}$ erg s^{-1}, $\gamma_w = 10$ and $\sigma = 0.1$, inside a 35-M$_\odot$ progenitor star. From left to right: density (g cm^{-3}), pressure (g cm^{-3} c^2) and velocity (in units of c). From top to bottom: snapshots at 4, 5 and 6 s after core bounce. Distances are in 10^9 cm; the radius of the progenitor star is 2.5×10^{10} cm. By $t = 5$ s (middle panel) the jet has escaped the progenitor star.

the high bounding pressure of the MWN. Even though the energy flux in the freely expanding wind is isotropic, the termination shock itself is highly asymmetric, with the radius of the termination shock being significantly smaller along the pole. Physically, this is because the strong toroidal field in the MWN creates an anisotropic pressure distribution with the pressure at the pole significantly larger than that at the equator (Begelman & Li 1992; Bucciantini et al. 2007). The higher polar pressure in turn causes the termination shock to be at a smaller radius. For the simulations in Figs 1 and 2, with $\sigma = 0.1$ in the wind, we find that the equatorial termination shock always lies outside $\approx 10^8$ cm. Thus our injection of a super-magnetosonic wind is self-consistent. By contrast, in simulations with a larger value of σ in the wind, we found that the termination shock can move in to $\lesssim r_{\rm min} = 10^7$ cm. Because the termination shock would then lie within the Alfvén surface, the spindown of the magnetar would be modified and our assumption of super-magnetosonic injection would be invalid. We defer a more detailed study of this interesting possibility to future work.

In the post-termination shock region, Fig. 2 shows that the flow undergoes a large-scale circulation with much of the matter being

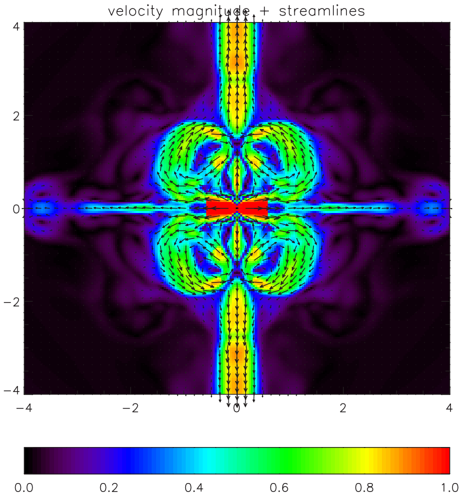

Figure 2. Inner velocity structure (in units of c) at 4 s after core bounce. Distances are in 10^9 cm. The termination shock is closer to the source along the pole because the pressure in the bubble is larger at the pole than at the equator. The flow pattern beyond the termination shock shows the formation of an axial jet/plume due to magnetic hoop stresses. Because the magnetic field goes to zero at the equator by symmetry, there is a small region of the equator where material can escape in an equatorial channel. This has no effect on the evolution of the system.

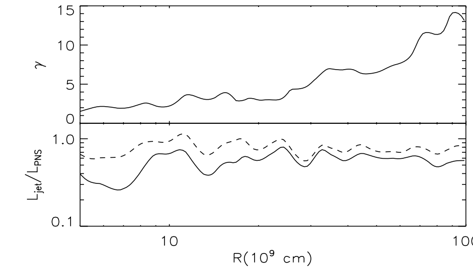

Figure 3. Upper panel: Lorentz factor on the axis of the jet, 9 s after core bounce for $\gamma_{\rm w} = 25$ and $r_{\rm max} = 10^{11}$ cm. γ increases roughly linearly in radius. Lower panel: ratio of the radial energy flux in the high-velocity core of the jet to the total source power (solid line). Also shown is the ratio of the total radial energy flux in the cocoon with respect to the source power (dashed line).

diverted from the equatorial region to the pole where it flows out along the jet, just as in analogous calculations for the structure of PWNe (Komissarov & Lyubarsky 2004; Del Zanna et al. 2004). This is caused by the toroidal magnetic field that builds up in the MWN, which is nearly in equipartition near the location where the back-flow starts (Del Zanna et al. 2004). Although collimation by hoop stresses is ineffective for the initially relativistic flow in the free wind, the non-relativistic $v \sim 0.5\,c$ flow in the post-termination shock region is effectively collimated by the magnetic field.

The MWN forms in about a sound crossing time $\sim$ 0.1–0.2 s. It takes $\sim$1 s for the magnetar to fill the MWN with enough energy for the magnetic stresses to become dynamically important, and about 1 more second for the jet/plume to emerge from the SN shock, still inside the star. The anisotropic pressure distribution in the MWN, with a much larger pressure at the pole than at the equator, and the significant energy and momentum flux in the axial jet act in concert to push out through the surrounding star along the polar direction. At $t = 4$ s, the MWN and jet are still fully contained within the star (Fig. 1). By $t = 5$ s, however, they have reached the radius of the star at $\approx 2.5 \times 10^{10}$ cm, and at $t = 6$ s the material in the jet at large radii has escaped the star and has accelerated back up to $v \approx c$. Note that the high-velocity core of the jet is surrounded by a cocoon of less relativistic material that includes shocked stellar wind material, as is generically expected to be the case (Uzdensky & MacFadyen 2006). The opening angle of the high-γ core of the jet is a few degrees. Because the jet is only marginally resolved in our fiducial simulations, we ran a higher resolution simulation with twice the number of grid points in the θ-direction near the axis of the jet; the results were nearly identical to those described here.

Although the magnetic field is crucial for generating and collimating the outflow seen in Fig. 1, the field is not energetically dominant; the ratio of the magnetic energy to the thermal energy in the bubble is typically $\sim$ 0.1–0.2, although it can reach $\sim$1 in the region where the hoop stress is most effective (Fig. 2). The enthalpy of the shocked gas in the post-termination shock region primarily determines the asymptotic Lorentz factor in the jet. In turn, the enthalpy of the shocked gas is determined (through the thermalization by the termination shock of the magnetar wind) by the wind Lorentz factor just upstream of the termination shock, $\gamma_{\rm w}$. Thus we find a roughly one-to-one relation between the Lorentz factor of the jet core at large radii and $\gamma_{\rm w}$: for $\gamma_{\rm w} = 10$ and $r_{\rm max} = 5 \times 10^{10}$ cm, γ reaches $\approx$5 in the jet, whereas for $\gamma_{\rm w} = 25$ and $r_{\rm max} = 10^{11}$ cm, $\gamma \approx 15$ at large radii. The upper panel in Fig. 3 shows γ on the axis of the jet as a function of radius for this simulation (at $t = 9$ s), demonstrating the acceleration from the marginally relativistic plasma at small radii near the termination shock to the highly relativistic flow with $\gamma \approx \gamma_{\rm w}$ at large radii. The acceleration is roughly linear in radius, consistent with that expected in a 'fireball' with a constant opening angle.

The lower panel in Fig. 3 shows the ratio of the power in the high-velocity core of the jet (solid) and in the wider cocoon (dashed) relative to the power supplied by the central source $\dot{E}$; as in the upper panel, these calculations are for $\gamma_{\rm w} = 25$ at $t = 9$ s when the outflow has escaped the star. Fig. 3 shows that at late times nearly all of the energy supplied by the central magnetar escapes to large radii and that a significant fraction of the energy is carried by the high-velocity core of the jet.

The upper and lower panels of Fig. 3 demonstrate radial fluctuations in the Lorentz factor and $\dot{E}$, respectively, despite the fact that the central source is assumed to have an $\dot{E}$ and $\gamma_{\rm w}$ that are constant in time. These fluctuations arise largely from shear instability near the base of the jet, and changes in the circulation of matter in the MWN (the region seen in Fig. 2) – this accounts for the characteristic length-scale of $\sim 10^9$ cm in Fig. 3. The corresponding variability time-scale is $\sim$ 0.01–0.1 s.

4 DISCUSSION AND IMPLICATIONS

Our simulations demonstrate that a wind with properties typical of proto-magnetar winds inside a massive star can be collimated into an axial jet, even in the conservative case in which the host star and wind are spherically symmetric. Physically, this occurs because of the strong toroidal magnetic field in the bubble of relativistic plasma and magnetic field that is at first inertially confined by the progenitor star and SN shock. The magnetic field creates an asymmetric pressure distribution in the bubble, with the pressure much larger at the pole than at the equator. In addition, the toroidal field collimates the moderately relativistic flow behind the termination shock into an axial jet.

Although we have not been able to carry out simulations with Lorentz factors of ~ 100–10^3 (largely for numerical reasons), as is required to explain GRBs, extrapolating our results suggests that an isotropic or equatorial flow with $\gamma \sim 100$–10^3 would produce a jet at large radii with a comparable Lorentz factor. This collimated outflow would thus have physical properties similar to those required to produce GRBs. As noted in Section 1, calculations of the mass-loss rate from newly formed magnetars find that magnetar winds naturally have $\sigma_{\rm LC} \gtrsim 100$–$10^3$ roughly 10–100 s after core bounce (Thompson et al. 2004; Metzger et al. 2007).

Fig. 3 shows that the jet escaping the star at large distances has fluctuations in γ and $\dot{E}$ on ~ 0.01–0.1 s time-scales. It is natural to speculate that this variability in the source region could manifest itself as variability in the gamma-ray emission in GRBs (via e.g. internal shocks). This is in addition to any intrinsic variability in the spindown of the central magnetar. It is also worth noting that the magnetic field in the MWN will be advected out to large radii where the GRB emission occurs (Lyutikov & Blandford 2003); the resulting field is likely strong enough to account for the observed gamma-ray emission via synchrotron radiation, without the need for shock-generated magnetic fields.

This Letter has focused on one part of the parameter space of proto-magnetar and host star interactions, namely a magnetar wind with $\sigma \sim 0.1$ spinning down into a cavity evacuated by a successful core-collapse SN. We find that in simulations with a more strongly magnetized wind ($\sigma \gtrsim 0.1$), the termination shock moves inside the Alfvénic and fast magnetosonic surfaces (Section 3). The spindown of the central magnetar will thus be modified. It is clearly of considerable interest to understand the coupled dynamics of the magnetar wind and the surrounding nebula in this limit. In addition, in our current simulations, nearly all of the spindown power of the central magnetar is channelled through the polar jet (Fig. 3). Thus the late-time spindown of the magnetar can likely generate a GRB, but it will not energize the surrounding SN. It is thus not clear if the current model produces *both* a hyper-energetic SN and a GRB, as is observed (Woosley & Bloom 2006). One possibility is that the initial explosion itself is highly energetic because rotational energy contributes to the explosion (e.g. Thompson, Quataert & Burrows 2005). Alternatively, we speculated in Bucciantini et al. (2007) that because the initial magnetar wind is likely to be significantly mass-loaded and non-relativistic, it may contribute to energizing the SN shock rather than to producing a GRB. This possibility will be investigated in future work with simulations that properly take into account the evolution of $\dot{E}$ and σ with time in magnetar winds. Finally, it is clearly important to understand the stability of the strong toroidal field that is crucial to the dynamics of the MWN and the axial jet. This can be studied both analytically and with 3D simulations.

Near the completion of this work, Komissarov & Barkov (2007) submitted a paper on magnetar spindown inside a star the results of which are complementary to ours. They calculated the dynamics of an outflow from a magnetar interacting with an infalling stellar progenitor for 200 ms after core-collapse, finding a collimated non-relativistic jet-like outflow. By contrast, we inject a super-magnetosonic wind with properties derived from separate spindown calculations, and are thus able to simulate the evolution for a much longer period of time, ∼10 s, and to much higher Lorentz factors. Although a number of the details differ, the broad conclusions from these two works are similar: magnetar formation can produce a jet with properties similar to those required to produce GRBs.

ACKNOWLEDGMENTS

NB was supported by NASA through Hubble Fellowship grant HST-HF-01193.01-A, awarded by the Space Telescope Science Institute, which is operated by the Association of Universities for Research in Astronomy, Inc., for NASA, under contract NAS 5-26555. EQ and BDM were supported by the David and Lucile Packard Foundation and a NASA GSRP Fellowship to BDM. JA's research has been supported by NSF grant AST-0507813, NASA grant NNG06GI08G and DOE grant DE-FC02-06ER41453, all at UC Berkeley; by the Department of Energy contract to the Stanford Linear Accelerator Centre No. DE-AC3-76SF00515; and by the taxpayers of California. We thank A. Heger for making massive stellar progenitor models available online.

REFERENCES

Begelman M. C., Li Z., 1992, ApJ, 397, 187
Bucciantini N., Thompson T. A., Arons J., Quataert E., Del Zanna L., 2006, MNRAS, 368, 1717 (B06)
Bucciantini N., Quataert E., Arons J., Metzger B. D., Thompson T. A., 2007, MNRAS, 380, 1541
Del Zanna L., Bucciantini N., 2002, A&A, 390, 1177
Del Zanna L., Bucciantini N., Londrilo P., 2003, A&A, 400, 397
Del Zanna L., Amato E., Bucciantini N., 2004, A&A, 421, 1063
Komissarov S. S., Lyubarsky Y. E., 2004, MNRAS, 349, 779
Komissarov S. S., Barkov M. V., 2007, MNRAS, in press (doi:10.1111/j.1365-2966.2007.12485.x) (arXiv:0707.0264)
Königl A., Granot J., 2002, ApJ, 574, 134
Lyubarsky Y. E., Eichler D., 2001, ApJ, 562, 494
Lyutikov M., Blandford R., 2003, astro-ph/0312347
MacFadyen A. I., Woosley S. E., 1999, ApJ, 524, 262
Matzner C. D., 2003, MNRAS, 345, 575
Metzger B. D., Thompson T. A., Quataert E., 2007, ApJ, 659, 561
Rhoads J. E., 1999, ApJ, 525, 737
Sherwin B. D., Lynden-Bell D., 2007, MNRAS, 378, 409
Thompson C., 1994, MNRAS, 270, 480
Thompson T. A., Chang P., Quataert E., 2004, ApJ, 611, 380
Thompson T. A., Quataert E., Burrows A., 2005, ApJ, 620, 861
Usov V. V., 1992, Nat, 357, 472
Uzdensky D. A., MacFadyen A. I., 2006, ApJ, 647, 1192
Uzdensky D. A., MacFadyen A. I., 2007, ApJ, 669, 546
Wheeler J. C., Yi I., Höflich P., Wang L., 2000, ApJ, 537, 810
Woosley S. E., Bloom J. S., 2006, ARA&A, 44, 507
Woosley S. E., Weaver T. A., 1995, ApJS, 101, 181
Woosley S. E., Heger A., Weaver T. A., 2002, Rev. Mod. Phys., 74, 1015

This paper has been typeset from a TEX/LATEX file prepared by the author.